



Part II Applied Physics

**Section 1 Atomic, Molecular and Optical
Physics**

Section 2 Plasma Physics

Section 3 Electromagnetics

Section 4 Radio Astronomy

Section 1 Atomic, Molecular and Optical Physics

Chapter 1 Quantum Optics and Photonics.

Chapter 2 Basic Atomic Physics.

Chapter 3 Molecular Physics.

Chapter 4 Small Angle X-Ray and Neutron Scattering —
Its Application to Supramolecular Solutions.

Chapter 1. Quantum Optics and Photonics

Academic and Research Staff

Professor Shaoul Ezekiel, Dr. Philip R. Hemmer, Dr. Mara G. Prentice, Dr. Horatio Lamela-Rivera, Bruce Bernacki, John Kierstead, Dr. Elias Snitzer

Graduate Students

Robert Barat, M. Selion Shahriar, Stephen P. Smith, Farhad Zarinetchi, John Donoghue

Sponsors

Charles Stark Draper Laboratory
 Joint Services Electronics Program (Contract DAAL03-86-K-0002)
 National Science Foundation (Grant PHY 82-10369)
 U.S. Air Force - Office of Scientific Research (Contract F49620-82-C-0091)
 U.S. Air Force - Rome Air Development Center

1.1 Laser Raman Clock Studies

We are continuing our precision studies of stimulated resonance Raman interaction in an atomic beam to determine its applicability to clocks and to demonstrate any advantages over conventional (microwave excited) atomic clocks. Up to this point, we have achieved a stability of 1×10^{-11} for a 5000 second averaging time using a sodium beam and a dye laser. This time compares favorably with commercial cesium clocks after differences in atom transit time and transition frequency are taken into consideration.

The stimulated resonance Raman process is illustrated in figure 1a in which we show a Raman transition between two long-lived states, 1 and 3, induced by two laser fields at frequencies ω_1 and ω_2 . These two laser fields are generated from the same laser to reduce the effects of laser jitter. It is well known that the Raman transition linewidth for weak, copropagating laser fields is primarily determined by the decay rates of the long-lived states 1 and 3. Therefore, the linewidth is set by the transit time. To achieve an effectively long transit time and a very narrow linewidth, Ramsey's technique of separated field excitation is used (figure 1b). Figure 1c shows a typical Raman-Ramsey fringe pattern obtained with a sodium beam and a dye laser. The central fringe linewidth in this data is 2.3 kHz, which is consistent with the

transit time. The Raman clock is simply a microwave oscillator stabilized to the central Raman-Ramsey fringe.

1.1.1 Ramsey Fringes in a Cesium Beam Using a Semiconductor Laser

Recently, we observed an ultra-narrow, 1 kHz (FWHM) wide Raman-Ramsey fringe in a cesium atomic beam with a 15 cm interaction zone separation and semiconductor laser with a free running linewidth of 20 MHz. Our observation showed us that it might be possible to develop a smaller, simpler, and less expensive clock based on the resonance Raman effect in cesium with a semiconductor laser.

The signal to noise ratio of the observed Ramsey fringes, shown in figure 2, is about 400 : 1 for a 1 second time constant. This is about ten times smaller than the shot noise limit expected for the present setup. The large fluorescence background and the fluorescence intensity fluctuations caused by the large degree of laser frequency jitter are the primary causes of the lower signal to noise ratio. Semiconductor lasers, which use optical feedback techniques and with frequency jitters on the order of 1 MHz, could reduce intensity fluctuations. To minimize the fluorescence background, we will shield the interaction region magnetically so that the $m = 0, \Delta m = 0$ Ramsey fringe will be

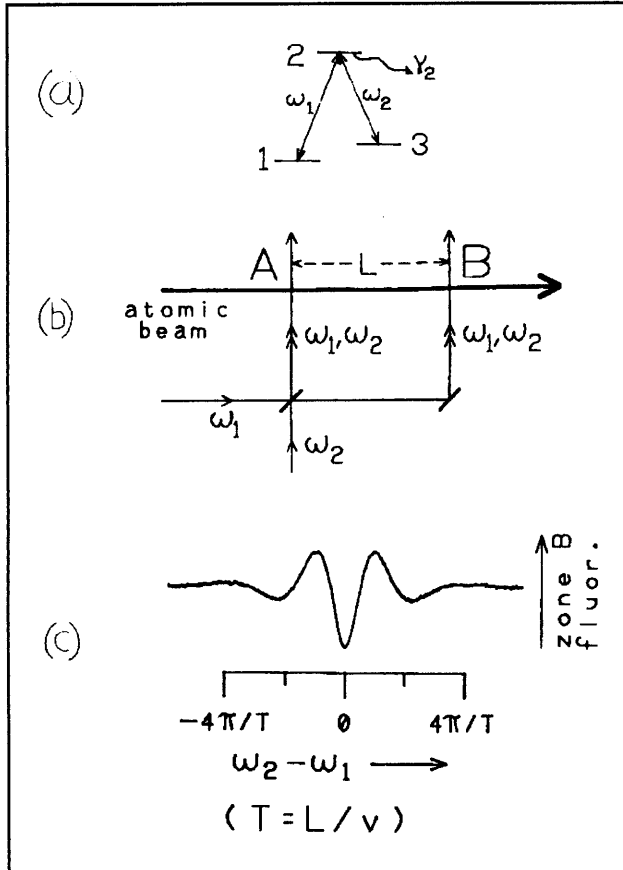


Figure 1. (a) Schematic of stimulated resonance Raman transition, γ_2 is the linewidth of the intermediate state. (b) Schematic configuration of the separated fields Raman interaction. (c) A typical Raman-Ramsey fringe pattern. T is the transit time in the separated fields interaction.

centered in a dip in the fluorescence. This dip is produced by several overlapping single zone Raman transitions between different m levels in a manner similar to the way it is produced in the sodium system. If we assume shot-noise limited detection, the fractional frequency stability would be $3 \times 10^{-11}/\tau^{1/2}$. This would compare well with commercially available cesium clocks. The signal to noise ratio could be improved further by increasing the atomic beam throughput, a practice which is currently being studied in optically pumped cesium clocks.

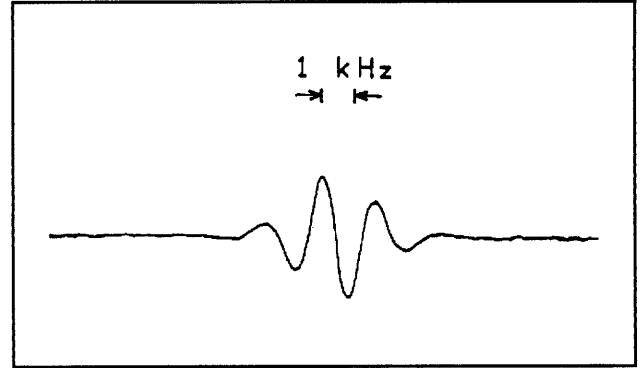


Figure 2. Raman-Ramsey fringes in a cesium atomic beam, obtained using a semiconductor laser with a free running linewidth of 20 MHz. The linewidth (FWHM) is 1 kHz, consistent with the transit time for a 15 cm zone separation and a 200 degree C oven temperature. The signal to noise ratio is 400.

1.1.2 Error Sources in a Sodium Raman Clock

Some of the error sources in a Raman clock are similar to those found in microwave clocks and include the effects of shifting path length, external magnetic fields, background slope, atomic beam misalignment, and second-order Doppler. Other sources of errors are unique to the Raman clock and include laser frequency detuning, laser intensity changes, optical pumping variations, laser beam misalignment, optical atomic recoil, and the presence of nearby hyperfine levels.

1.1.3 AC-Stark Shifts in a Two-Zone Raman Interaction

Our expanded study of laser detuning effects (common mode) include other effects in addition to those from optical resonance that might occur, for example, because of misalignment of beams. This detuning causes the fringe minimum to shift in frequency as a manifestation of the AC-Stark effect. Previously, we performed preliminary theoretical and experimental investigations into the results from this effect. We found that the shift depends on the amount of detuning, the laser intensity, and the population difference between the ground levels before the interaction began.

We extended our investigations of the AC-Stark shift to consider the effects of laser intensity in greater detail and also to deter-

mine the role of Zeeman sublevels. For example, we found experimentally that the AC-Stark shift is almost insensitive to the variation of the ratio of the intensities of the laser fields at the two frequencies as long as the sum of the intensities remains unchanged. When the theoretical expression for the AC-Stark shift was extended to include the case of unequal intensities, the degree of insensitivity was predicted correctly (figure 3). This observation is unexpected when the three level system is considered to be two independent two-level systems.

We also predicted theoretically that the AC-Stark shift does not depend strongly on the exact laser intensity profile as long as the time integrated intensity experienced by the moving atom remains unchanged. In a two level system, this would be analogous to the equivalent, for example, of two π pulses of different shapes, where π is the time integral of the square root of the laser intensity (in units of Rabi frequency) as experienced by the atom. This predicted insensitivity to laser profile has been verified experimentally (figure 4).

Finally, we have augmented the theory of the Raman interaction in an ideal three level system to account for the effects of the additional Zeeman sublevels. We have accounted for these effects to first order by introducing effective within-system decay rates to the closed three level system equations. Such an augmented anomalous has successfully predicted an experimentally observed anomalous slope reversal in the AC-Stark shift as a function of detuning.

The slope reversal mentioned above can be achieved by varying laser intensity or the initial population difference between the ground states. This implies that for a set of values of these parameters, the slope becomes small. Figure 5a shows a high resolution experimental plot of the AC-Stark shift versus laser detuning obtained under conditions that are experimentally determined to minimize the slope of the AC-Stark shift. This data is shot noise limited and was obtained with an averaging time of 1 sec. As can be seen, the AC-Stark shift is less than the noise over a laser detuning of $\pm 0.2\gamma_2$ where γ_2 is the linewidth of the intermediate level. In comparison, figure 5b shows the

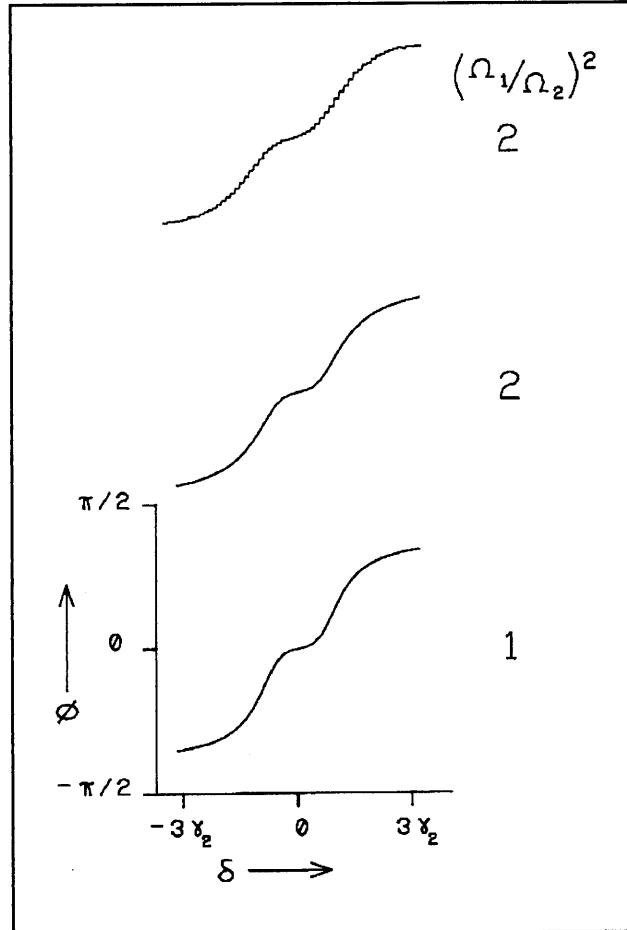


Figure 3. Illustration of insensitivity of AC-Stark shift to differences in Rabi frequencies. (Top trace) Data showing AC-Stark shift for unequal Rabi frequencies, $|\Omega_1/\Omega_2|^2 = 2$. (Middle trace) Theoretical AC-Stark shift for $|\Omega_1/\Omega_2|^2 = 2$. (Bottom trace) Theoretical AC-Stark shift for $|\Omega_1| = |\Omega_2|$ but the same $(|\Omega_1|^2 + |\Omega_2|^2)$. Here, Ω_1 and Ω_2 are the Rabi frequencies corresponding to the 1-2 and 3-2 transitions, respectively. δ is the common mode laser detuning, and ϕ is the AC-Stark shift, where $\phi = \frac{\pi}{2}$ corresponds to a shift of half the linewidth (FWHM) of the Ramsey fringe.

theoretical AC-Stark shift under experimental conditions in which the effective within-system decay rates have been used as a free parameter to produce the flattest trace. Good agreement between theory and experiment is clearly achieved when the effect of the Zeeman sublevels is taken into account by this one parameter fit.

It should be noted that the suppressed AC-Stark shift of figure 6 (clock stability of better than 2×10^{-11} for a laser detuning of $0.01 \gamma_2$) is still preliminary and does not represent the ultimate achievable clock perform-

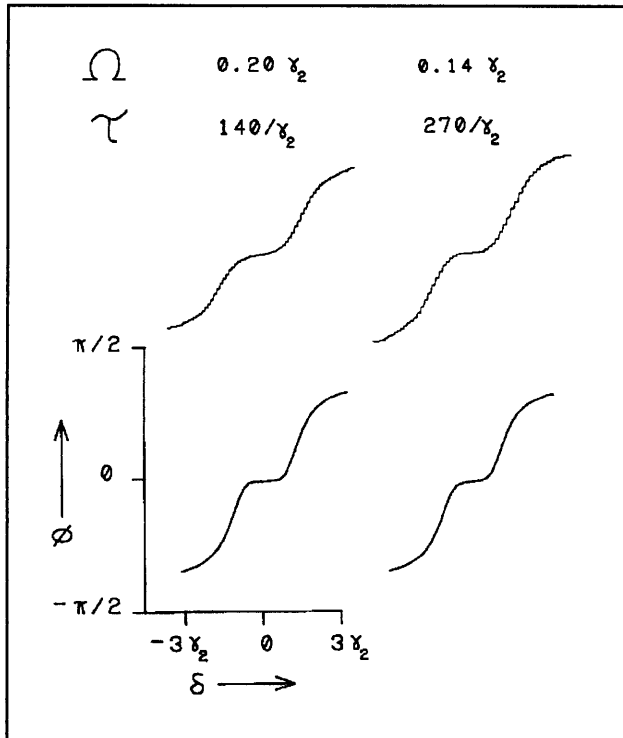


Figure 4. Illustration of insensitivity of the AC-Stark shift to the exact laser beam profile. First interaction zone transit times, τ , are as indicated ($\Omega^2\tau$ remains constant, where Ω^2 is the average (squared) Rabi frequency). Top traces are experimental, bottom traces are theory.

ance. In the future, we plan to verify that the AC-Stark shift could be further suppressed by increasing the degree of Raman saturation. This could be achieved by either increasing the laser intensity, or by slowing down the atoms (by cooling, for example). In addition, numerical calculations are in progress to identify the exact role played by the Zeeman sublevels.

1.1.4 Reduction of Background Slope Effects

Another important source of error is the background slope of the Raman-Ramsey fringe pattern. A variation in this slope, which might occur due to a change in the laser intensity, corresponds to a shift in the clock frequency. One way to reduce this effect is to use the third, instead of first, harmonic of the modulation frequency in the phase sensitive demodulation. In general, third harmonic demodulation is accompanied

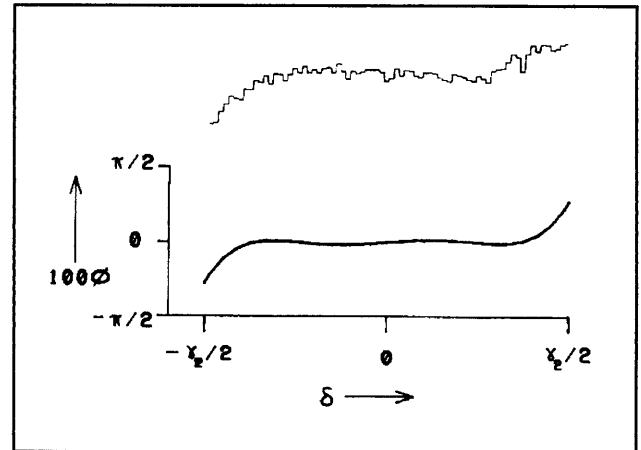


Figure 5. High resolution AC-Stark shift vs. laser detuning: (a) Experimental trace for $\Omega = 0.13\gamma_2$, $(\rho_{11} - \rho_{33})/N = 0.7$ (normalized initial population difference), and (b) Corresponding theoretical best fit, with $r' = 0.27$, where r' is the normalized difference of the effective within-system decay rates.

by a reduction in the signal to noise ratio of at least 3, thus reducing the short term stability. However, we have shown, experimentally as well as through numerical simulation, that for the case of Raman-Ramsey fringes, the reduction in the signal to noise ratio is less than a factor of 2 because of the unique shape of the Ramsey fringe pattern. Therefore, the resulting reduction in the short term stability using the third harmonic is much less than expected, and the increase in the long term stability is preserved. Our experimental determination of the amount of increase in the long term stability is in progress.

Publications

Hemmer, P.R., M.S. Shahriar, V.D. Natoli, and S. Ezekiel "AC-Stark Shifts in a Two Zone Raman Interaction," accepted for publication in *J. Opt. Soc. Am. B*.

Hemmer, P.R., H. Lamela-Rivera, S.P. Smith, B.E. Bernacki, M.S. Shahriar, and S. Ezekiel, "Observation of Ultra-Narrow Ramsey Raman fringes in a Cesium Atomic Beam Using a Semiconductor Laser," submitted to *Optics Lett*.

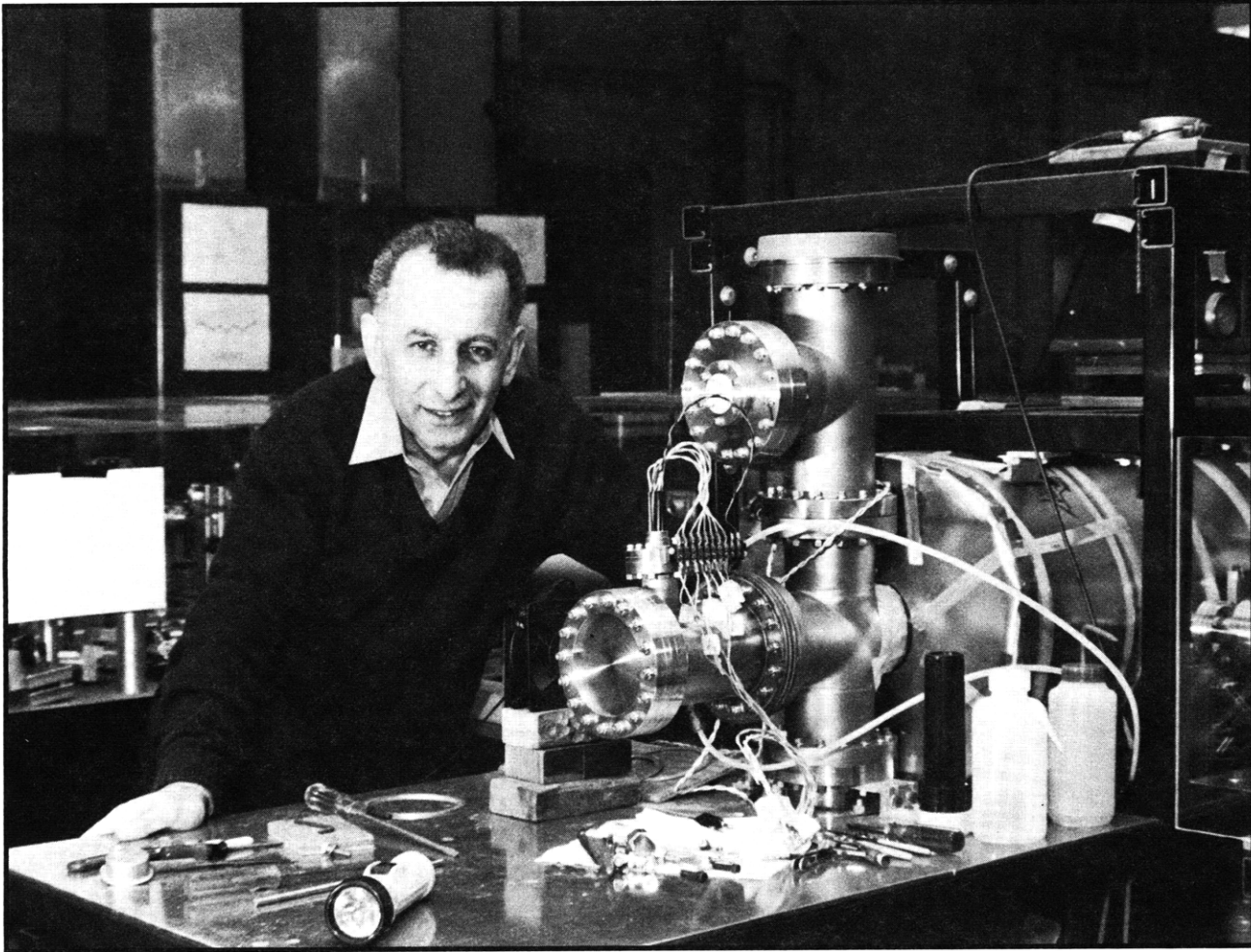
Shahriar, M.S., *Raman Clock Studies*, S.M. thesis, Dept. of Electr. Eng. and Comp. Sci., MIT, 1989.

1.2 Fiberoptic Gyroscope Studies

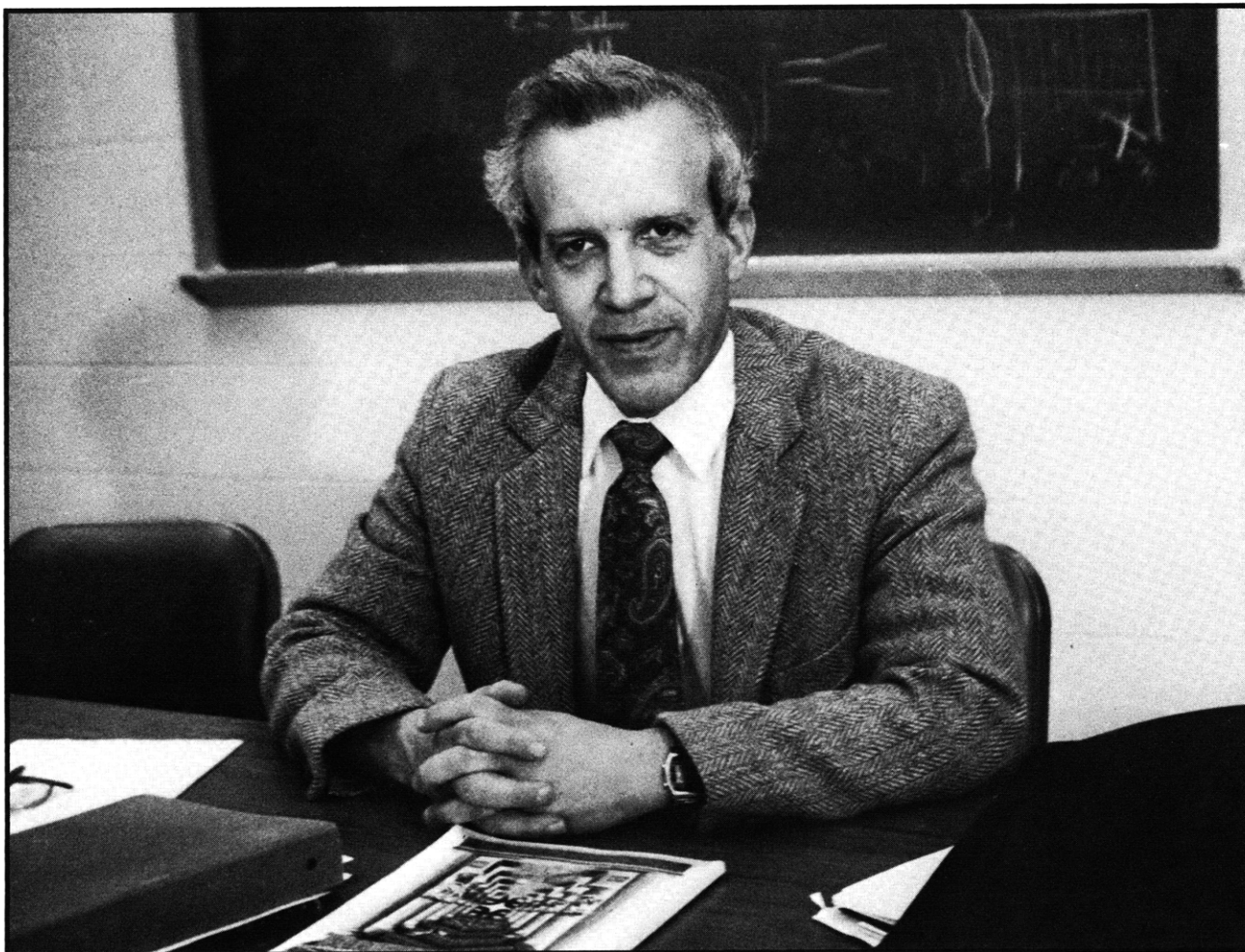
We are studying a variety of issues concerning the performance of a fiberoptic resonator gyroscope. In particular, we observed stimulated Brillouin scattering and are examining its effect on gyro behavior and performance. Furthermore, we have been studying the feasibility of a fiber laser gyroscope based on Brillouin scattering.

1.3 Laser Linewidth Narrowing

Single frequency semiconductor lasers exhibit a rather broad spectral width in comparison with other lasers. Many techniques have been developed for reducing the linewidth of semiconductor lasers. These techniques include use of optical feedback and placement of the laser in an external cavity. Our linewidth narrowing technique is based on stimulated Brillouin scattering in a fiber. Our preliminary experiments have shown that it is possible to achieve very narrow linewidths of less than a few Hertz with a good conversion efficiency.



Professor Shaoul Ezekiel



Professor Daniel Kleppner